Analysis of the Effects of Vertical Pre-Release Cracks on Prestressed Concrete Bridge Girders

Eray Baran
Graduate Student
Civil Engineering Department
University of Minnesota
Minneapolis, Minnesota

Carol K. Shield, Ph.D., P.E.
Associate Professor
Civil Engineering Department
University of Minnesota
Minneapolis, Minnesota

Catherine E. French, Ph.D., P.E.
Professor
Civil Engineering Department
University of Minnesota
Minneapolis, Minnesota

Tina A. Wyffels, P.E.
Structural Engineer
BKBM Engineers
Minneapolis, Minnesota

Vertical cracks, termed "pre-release cracks," beginning at the top flange and propagating downward into the section depth have been observed to develop during the production of long-span prestressed concrete bridge girders. The cracking, which is attributed to the restrained shrinkage of the concrete and thermal effects during the curing period prior to release of the prestressing strands, tends to be more critical for long-span girders with deep sections and large amounts of prestressing strands. Studies were conducted at the University of Minnesota to investigate the effects of pre-release cracks on the behavior of bridge girders. The effects of the size of pre-release cracks on beam stresses and crack-closure behavior were studied with finite element models. Full-scale Mn/DOT Type-28M prestressed concrete bridge girders incorporating artificially-made pre-release cracks were tested under four-point bending to verify the findings. Closing of the pre-release cracks and the beam strains and deflections were monitored continuously during the load tests. The pre-release cracks were found to cause local changes in the beam strains near the crack locations. Beams with pre-release cracks were observed to undergo flexural crack initiation and crack re-opening at lower loads than similar beams without pre-release cracks.

As high strength concrete construction continues to become more popular, heavily reinforced sections with very long span lengths are being used for precast, prestressed concrete bridge girders. During production of these girders, it has been observed that vertical cracks may develop near the midspan of the girders if they are left on the casting bed for an extended period of time before releasing the prestressing strands.[1-5] Vertical cracks have been observed to initiate at the top flange and propagate downward in the section. In some cases, cracks have been observed to extend through the entire girder depth.

The reason for the cracking is attributed to restrained shrinkage and thermal effects during the curing period of the girders at precast facilities prior to release of the prestressing strands.[1,4,6] During the production of precast, prestressed girders, concrete shrinkage is restrained by the prestressing strands, hold-down attachments, and surface friction between the girders and the casting bed. In addition, contraction of the exposed strands occurs between the girders (due to rapid cooling after steam curing) creating extra tensile strains in the bonded concrete, which increases the likelihood of pre-release cracking.

Cracking problems are more critical for high strength concrete bridge girders due to longer span lengths and the incorporation of larger amounts of prestressing strand. The increased girder lengths often result in a decrease in the free length of strands in the precasting bed, and this combined with the increased strand area may contribute to increased girder restraint forces, and the consequent increased likelihood of pre-release cracking.

The pre-release cracks are often observed to close upon transfer of prestressing forces due to the compressive stresses resulting from prestress and self-weight. However, the cracks appear to have an impact on flexural cracking loads as observed in tests of long-span precast high strength concrete prestressed bridge girders conducted at the University of Minnesota.[1]

Two full-scale Mn/DOT 45M prestressed concrete girders were cast and tested by Ahlborn et al.[1] to investigate the use of high-strength concrete in prestressed bridge girders. Two girders were cast on the same bed. One of the girders reached the required concrete strength earlier than the other girder, and the forms for that girder were stripped. The girders were left on the bed without detensioning the prestressing strands while waiting for the other girder to reach the required release strength. During this period, pre-release cracks were observed to develop in the girder which had the forms stripped. In total, fifteen vertical pre-release cracks were observed to develop. These cracks initiated at the top of the girder and were concentrated within the middle 40 percent of the span length. The average crack depths ranged from 3.4 to 40.3 in. (86 to 1024 mm), and the cracks were observed to close completely following release of the prestressing strands. Decks were cast on each girder, and the girders were subsequently tested in flexure. At the time of testing, the uncracked and cracked girders were 594 and 725 days old, respectively.

Results from the static tests of the girders indicated a reduction in the flexural cracking capacity of the girder that had developed pre-release cracks. Initial flexural cracks were observed to occur outside the constant moment region in a four-point bending flexural test due to the effect of pre-release cracks. Moreover, the first six flexural cracks were observed to be within 18 in. (457 mm) (40 percent of girder depth) of a pre-release crack.

The tests were followed by a finite element study in which it was determined that pre-release crack closure causes local reductions in the compressive stress at the bottom of the girders in the vicinity of the pre-release cracks.[7] The reduced compressive stresses due to the existence of pre-release cracks lead to the onset of flexural cracking at those locations at load levels less than the predicted cracking loads.

To verify the findings from the finite element study, a companion experimental study was conducted on prestressed concrete girders incorporating artificially-made pre-release cracks. This paper describes the results of the experimental study and the companion finite element study.

FINITE ELEMENT STUDY

Description of Models

The effects of pre-release cracks have been investigated numerically through finite element models of 135 ft (41.1 m) long prestressed concrete girders with a 45 in. (1143 mm) deep, 22 in. (559 mm) wide rectangular cross section incorporating discrete pre-release cracks.[7] Two-dimensional finite element models, created with ABAQUS software,[8] were utilized. The beams were modeled with eight-node biquadratic reduced integration plane stress elements.

The prestressing strands inside the beams were modeled as linear truss elements with nominal area of the steel equivalent to forty-six 0.6 in. (15.2 mm) diameter strands. An initial stress that provided a total prestressing force of 3000 kips (13,350 kN) was assigned to the truss elements. This force corresponded to a strand stress that was greater than 75 percent of the specified tensile strength of the prestressing steel for Grade 270 strands.

A large prestressing force was used to cause the pre-release cracks to close completely in the models involving large crack widths and small crack depths. The truss elements were placed 9 in. (229 mm) up from the bottom of the beam so that the pre-release cracks would close completely in more of the models.

Gap elements that only transferred compressive forces in the horizontal direction were used to model the pre-release cracks with a V-shaped cross section. Several different pre-release crack depths [12, 24, and 33 in. (305, 610, and 838 mm)] (crack depths measured from the top of the beam) and widths [$^1/_{100}$, $^1/_{32}$, and $^1/_{16}$ in. (0.25, 0.79, and 1.59 mm)] (the maximum width at the top of the crack) were modeled to monitor the closure of the cracks and their effects on girder stresses.

The girder ends were modeled as simple supports. The self-weight was applied to the model as a uniformly distributed lineal load acting on the top surface of the model. The additional superimposed uniform load varied from 100 to 800 lb per ft (1.46 to 11.7 kN/m) with a 100 lb per ft increment and was applied to the model in a similar manner as the self-weight.

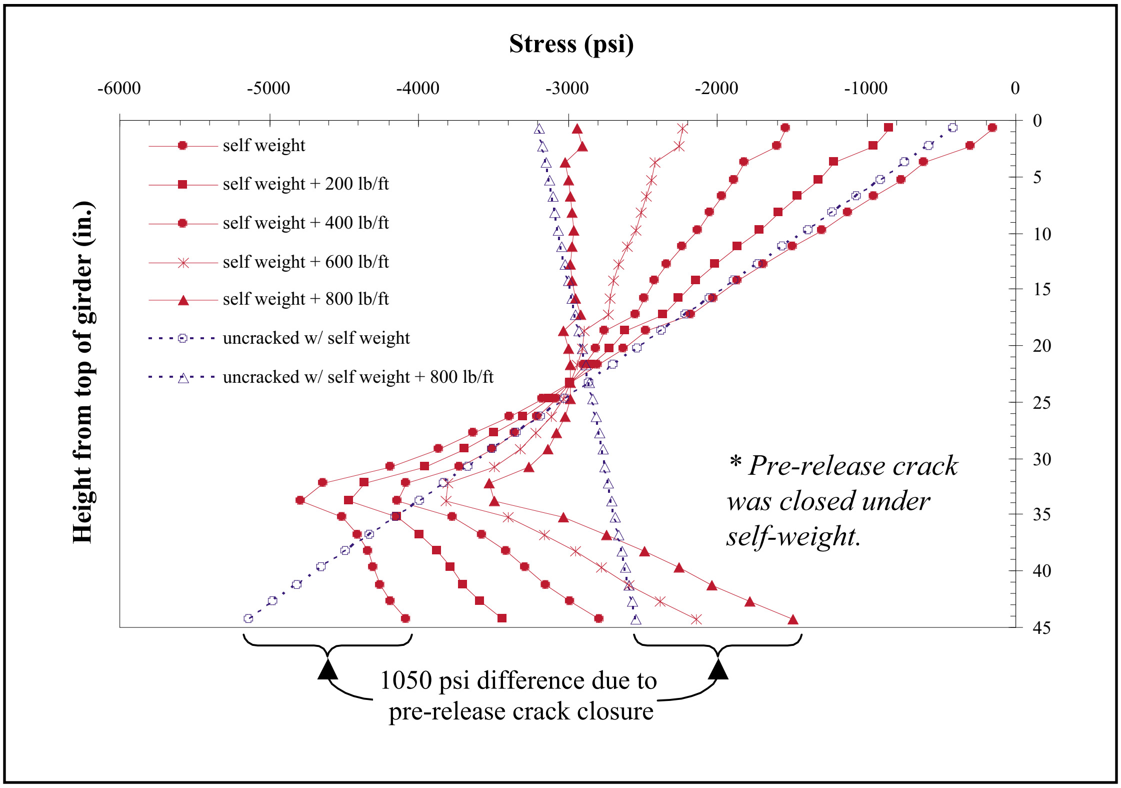

Fig. 1. Stress distributions due to 33 in. (838 mm) deep, 1/32 in. (0.79 mm) wide pre-release crack.

Results From Finite Element Models

Stress differences were observed in the models incorporating pre-release cracks compared to those of models without pre-release cracks. The differences in stresses were found to be local to the crack locations. The span length over which there was a change in stress state due to the existence of a pre-release crack was limited to a distance equal to the depth of the beam on each side of the crack location.

The stress changes included reductions in compressive stresses in the bottom fiber below the pre-release cracks and at the top of the cracks, and increases in the compressive stresses near the crack tip. It was also found that a nonlinear stress distribution occurred near the pre-release cracks during crack closure as a result of changing stiffness of the cross section.

After the cracks had completely closed, linear stress increments occurred with increasing load, due to the constant sectional stiffness during this loading phase until flexural cracking. However, these linear stress increments were superimposed on the nonlinear stress distribution, which became “locked in” to the section upon crack closure. The term “locked in” means the pre-release crack-induced effects on beam stresses exist after the cracks closed completely.

The reduced compressive stresses below the pre-release cracks resulted in lower flexural crack initiation and re-opening loads than those observed in the beams that did not have pre-release cracks. The reduction in compressive stresses below the pre-release cracks, and hence in the flexural crack initiation and re-opening loads of the beams, was due to two effects. Part of the reduction was attributed to closing of the pre-release cracks, and the remaining part was due to the reduced sectional stiffness at the pre-release crack locations when the cracks remained partially open at the flexural crack initiation and re-opening loads.

The process of closing the pre-release cracks due to the effects of the prestressing force, self-weight of the girders, and the externally applied loads caused additional superimposed tensile stresses to develop at the bottom of the girder in the vicinity of the crack during crack closure, which, in turn, resulted in reduced bottom fiber compressive stress.

A second reason for the reduction in the flexural crack initiation and re-opening loads of the beams with pre-release cracks was the reduced sectional stiffness at the pre-release crack locations in cases where the pre-release cracks remained partially open at flexural crack initiation and re-opening loads. If the pre-release cracks remained partially open, the section at the pre-release crack location had a reduced cross-sectional area and moment of inertia as compared to uncracked sections. The reduced moment of inertia at the location of the pre-release cracks resulted in increased superimposed tensile stresses at the bottom of the girders near the crack locations compared to other locations along the girder, which caused reductions in the flexural crack initiation and re-opening loads of the beams.

In general, shallower and wider pre-release cracks required larger loads to close completely than deeper and narrower cracks. Results from the models indicated that a major reduction in flexural cracking load occurred for the cases in which the pre-release cracks remained partially open at flexural crack initiation due to the reduction in gross moment of inertia. There were also cases in which the effect of the reduced bottom fiber compressive stress due to pre-release crack closure caused large reductions in compressive stresses at the bottom fiber of the section.

For example, Fig. 1 shows the stress distributions at the pre-release crack location for the model with a 1⁄32 in. (0.79 mm) wide and 33 in. (838 mm) deep crack. The pre-release crack in this model was observed to close completely under the effects of prestressing force and the self-weight of the girder only. As evident in the figure, a considerable reduction in the bottom fiber compressive stress below the pre-release crack occurred during the closure of the crack.

Closure of the pre-release crack due to the prestressing force and beam self-weight resulted in a nonlinear stress distribution through the section. This nonlinearity was "locked in" and existed in the stress distributions for all load levels shown in the figure, even though the crack had closed completely under the prestressing force and beam self-weight. Considering that Ahlborn[1] and Green et al.[4] reported pre-release crack widths of up to 0.025 and 0.04 in. (0.64 and 1.02 mm), respectively, the crack width of 1⁄32 in. (0.79 mm) used in this model was a good representation of pre-release crack widths observed in the field.

As shown in Fig. 1, there was an approximately 1050 psi (7.2 MPa) reduction in bottom fiber compressive stress of the model compared to the case with no pre-release crack under all values of externally applied load (including the case with no external load). This reduction, which is unacceptably large, indicates that pre-release cracks might cause significant stress changes even though they close under the effects of prestressing force and self-weight of the girder.

Table 1. Specimen details.

Series	Beam designation	Pre-release crack-former dimension		Number of pre-release cracks	Pre-release crack spacing
		Depth, in.	Width, in.		
Single crack series	SC-UC-1*	Uncracked			
	SC-UC-2	Uncracked			
	SC-UC-3	Uncracked			
	SC-06-08	6	0.008	1	n/a
	SC-06-14	6	0.014	1	n/a
	SC-16-08	16	0.008	1	n/a
	SC-16-14	16	0.014	1	n/a
	SC-22-08	22	0.008	1	n/a
	SC-22-14*	22	0.014	1	n/a
	SC-22-14-R1	22	0.014	1	n/a
	SC-22-14-R2*	22	0.014	1	n/a
Multiple crack series	MC-UC-1	Uncracked			
	MC-UC-2	Uncracked			
	MC-1C	16	0.014	1	n/a
	MC-3C-W	16	0.014	3	Widely
	MC-3C-C	16	0.014	3	Closely
	MC-3C-C-R	16	0.014	3	Closely

* Beams subjected to cyclic loading.
Note: 1 in. = 25.4 mm.

Table 2. Calculated midspan section stresses following release of prestressing strands.*

Series	Bottom fiber stress (compression), psi	Top fiber stress (tension), psi
Single crack series beams	980	280
Multiple crack series beams	860	130

* Section stresses are for a beam with no pre-release cracks.
Note: 1 psi = 0.006894 MPa.

EXPERIMENTAL STUDY

The experimental study included tests of 17 Minnesota Department of Transportation (Mn/DOT) Type 28M prestressed concrete beams, some of which had artificially-made pre-release cracks with different sizes. The two testing phases were static tests of single crack and multiple crack series beams, and cyclic tests of three of the single crack series beams.[9] The pre-release cracks were purposely made to facilitate placement of instrumentation used to compare the experimental and numerical results.

The terms "crack depth" and "crack width" used in this paper refer to the nominal pre-release crack dimensions, i.e., the depth and maximum width (at the top of the crack), respectively, of the crack formers used to produce the cracks in the test beams. The actual crack widths in the test beams may have been larger than these nominal crack widths due to such effects as the shrinkage of the concrete.

Additional two-dimensional finite element models of Mn/DOT Type 28M beams, created with ABAQUS software, were utilized for the optimization of the beam design, including beam lengths, amount of prestressing force, and pre-release crack dimensions and locations. Changes in beam strains obtained from these models were also compared with experimentally obtained values. The beams were fabricated at a local precasting yard and transported to the University of Minnesota Department of Civil Engineering Structures Laboratory in Minneapolis, where the tests were performed.

Description of Specimens

The specimens were divided into two series: single crack series beams and multiple crack series beams. Table 1 lists the test specimens and their associated variables. The single crack series beams consisted of eleven 20 ft

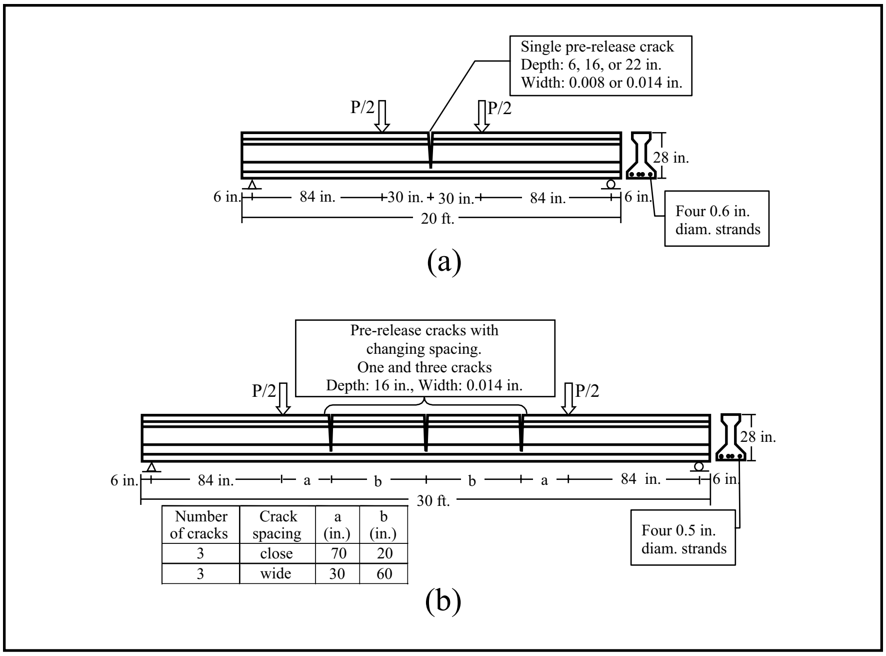

Fig. 2. Details of test beams: (a) single crack series beams; (b) multiple crack series beams.

(6.1 m) long beams incorporating four 0.6 in. (15.2 mm) diameter seven-wire Grade 270 prestressing strands initially tensioned to 54 percent of f_{pu}, where f_{pu} is the specified tensile strength of the prestressing steel.

The prestressing strands were straight and placed in one layer 2 in. (51 mm) from the bottom of the beams. Calculated top and bottom fiber stresses at release of prestressing strands at the midspan section of a beam with no pre-release cracks are given in Table 2.

Eight of the beams in this series incorporated a single pre-release crack at midspan with varying crack depths [6, 16 or 22 in. (152, 406 or 559 mm)] and crack widths [0.008 or 0.014 in. (0.20 or 0.36 mm)]. Three of the beams served as control specimens and thus did not have pre-release cracks.

The finite element study indicated that the span length over which the pre-release cracks had an effect on stresses was limited to the depth of the beam on each side of the crack, and that multiple pre-release cracks interact with each other when the affected stress areas of the cracks overlap. Multiple crack series beams, which were 30 ft (9.14 m) long and prestressed with four straight 0.5 in. (12.7 mm) diameter seven-wire Grade 270 strands placed in one layer 2 in. (51 mm) from the bottom of the beams, were used for the investigation of multiple pre-release crack interaction.

The prestressing strands in the multiple crack series beams were initially tensioned to 76 percent of the specified tensile strength of the steel so that these beams had a similar level of total prestressing force as the single crack series beams (section stresses at strand release are given in Table 2). Three of the six beams in this series incorporated three pre-release cracks with identical crack geometry, which were spaced either widely or closely. Fig. 2 shows the location of pre-release cracks and loading points in the beams. Pre-release cracks in the beams were placed inside the constant moment region, as shown in Fig. 2.

The beams were fabricated in two separate casts. The 20 ft (6.1 m) span beams were fabricated in the first cast. The second cast, produced six days later, consisted of the 30 ft (9.14 m) span beams. During the fabrication of the beams, standard construction techniques were used, except for the placement of crack-formers between the segments of the steel forms (see Fig. 3). Laminated plates made of 0.002 in. (0.05 mm) thick layers of steel sheets were used for the crack-formers.

The thickness of the crack-former was changed at several depths by peeling off layers of the plate to taper the crack with the tip of the crack former dimension being either 0.002 or 0.004 in. (0.05 or 0.1 mm) thick. The crack former plates were removed after the concrete hardened (1 to 2 hours after concrete casting). The concrete

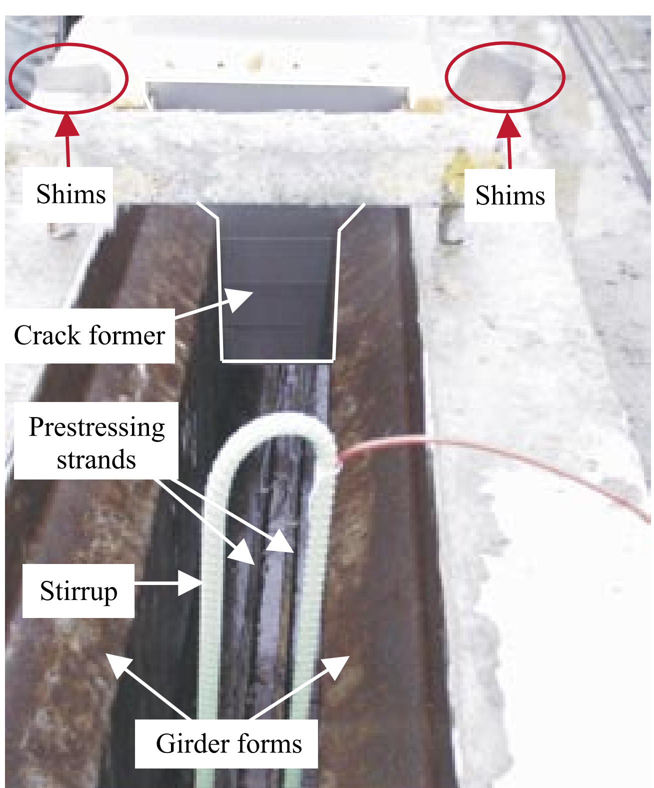

Fig. 3. Crack-former placed between girder forms.

mix used for the beams had a measured 28-day compressive strength of 9250 psi (63.8 MPa).

Measurements of pre-release crack widths were taken using feeler gauges prior to and following release of prestressing strands in an attempt to determine the original crack geometries. It was difficult, however, to obtain reliable measurements because of the effect of local changes in the crack openings, such as those due to irregular crack surfaces or particles stuck inside the crack.

As mentioned later with the test results, the pre-release cracks in the test beams did not close completely following the release of prestressing strands, in contrast to what is generally observed in the field. One of the reasons for this phenomenon was the relatively small self-weight moment of the beams due to the small cross-sectional area and short span length. Another reason for the large resistance against pre-release crack closure was the relatively large eccentricity of the prestressing force.

In the test beams, the prestressing strands were located only 2 in. (51 mm) from the bottom of the beam. In girders that are in service, the location of the center of gravity of prestressing strands is usually higher (i.e., the strand eccentricity is usually smaller). If the strands in the test beams had been located close to or coincident with the tip of the pre-release cracks, this configuration would cause difficulties during the construction of the beams in trying to locate the crack formers.

On the other hand, if the strands had been placed at a higher level in the beams to reduce the eccentricity and hence resistance to pre-release crack closure, then the depth of the deepest pre-release crack that could have been produced would have been reduced. That would have further limited the range of pre-release crack depths to be investigated in the study. As a result, a relatively large eccentricity was used with a small number of strands to reduce the resistance against pre-release crack closure and also to prevent initiation of additional cracking below the tip of the already existing pre-release crack.

The fact that the pre-release cracks in the test beams did not close completely following the release of prestressing strands provided the opportunity to monitor the progressive closing of the cracks during load tests.

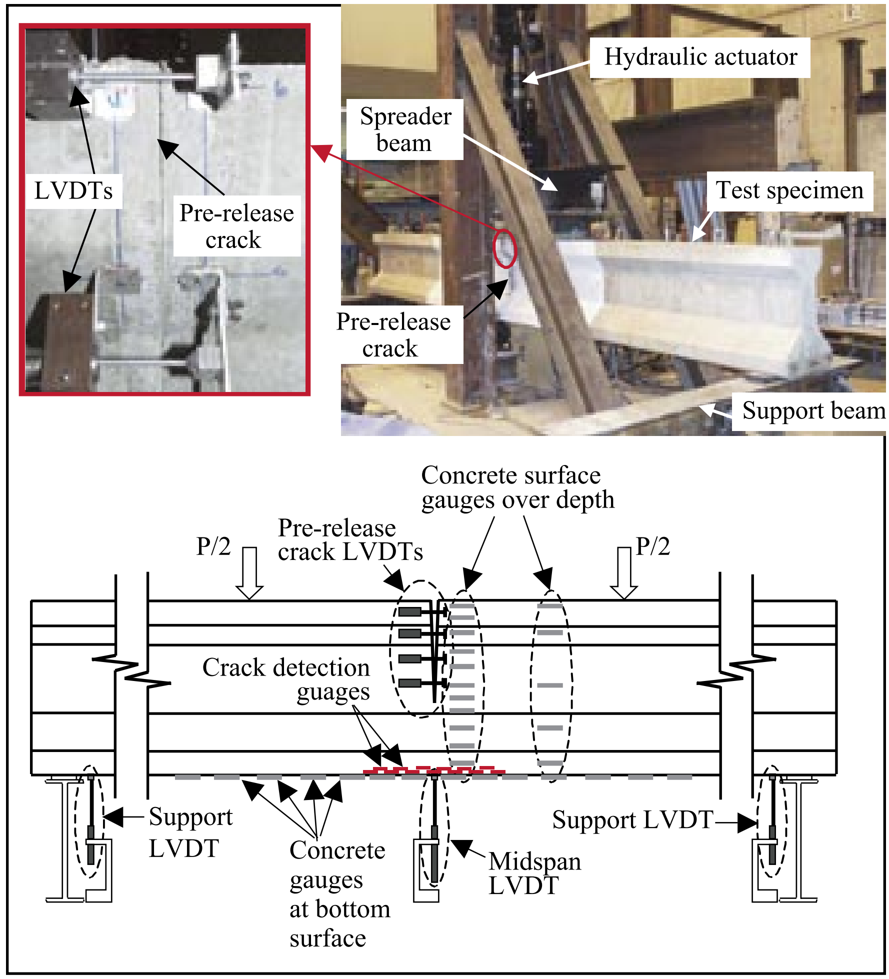

Fig. 4. Test setup and instrumentation scheme.

Instrumentation and Testing

The external instrumentation scheme is shown in Fig. 4. Pre-release crack closure was measured during the load tests using linear variable differential transformers (LVDTs) centered across the cracks at several locations along the crack depth. The beams were heavily instrumented with concrete surface strain gauges in the vicinity of the pre-release cracks both over the depth and along the length to capture local changes in strain distributions.

Typically, the strain gauges were placed on the bottom surface of the beams at 2 in. (51 mm) spacing in the vicinity of pre-release cracks and at 4 in. (102 mm) spacing elsewhere in the constant moment region of single crack series beams. Wider strain gauge spacings were used in multiple crack series beams. Using surface strain gauges with a relatively long gauge-length [2.36 in. (60 mm)] minimized the local effects of the concrete paste and aggregate on the measured strains.

Reliability of the measurements from the concrete surface gauges was verified by the electrical resistance gauges embedded in the concrete during the fabrication of the beams. Crack detection gauges were also mounted on the bottom flange near the pre-release crack locations in order to detect the flexural crack initiation.

The beams were simply supported at the ends by elastomeric bearing pads and tested flexurally under four-point bending with the pre-release cracks in the constant moment region, as shown in Figs. 2 and 4. The clear span was 19 ft (5.79 m) for the single crack series beams and 29 ft (8.84 m) for the multiple crack series beams. Each beam was subjected to a flexural crack initiation

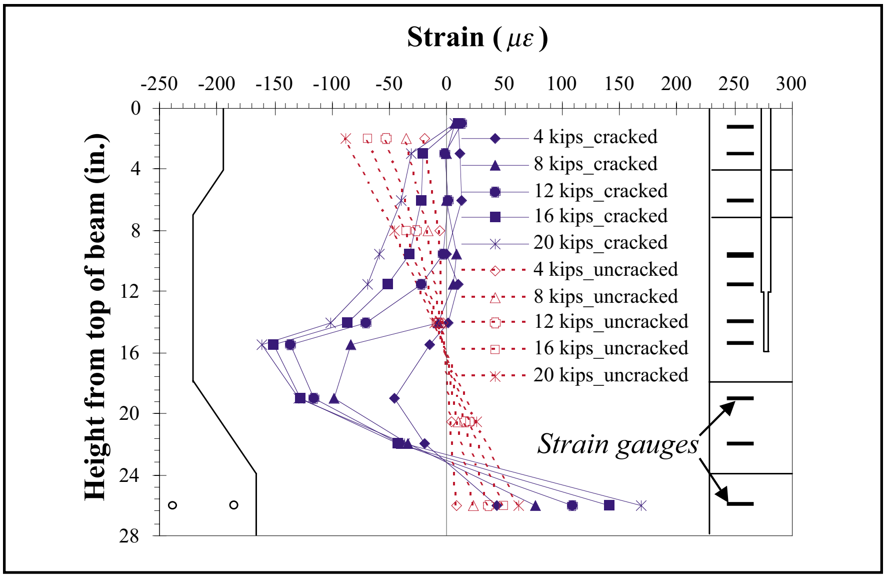

Fig. 5. Measured strain distributions near pre-release cracks at midspan (Beam SC-16-08) and at corresponding location in uncracked beam (Beam SC-UC-2).

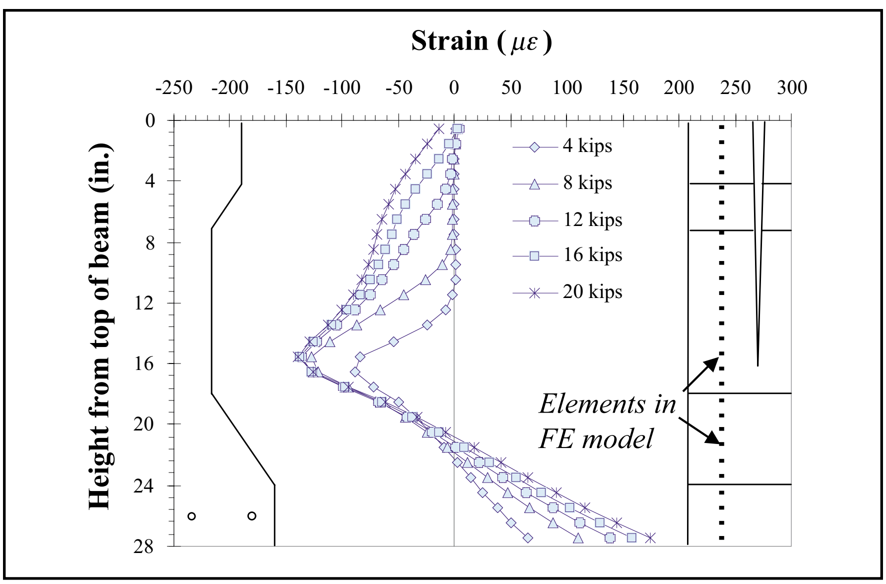

Fig. 6. Calculated strain distributions near pre-release crack at midspan (Beam SC-16-08).

test followed by crack re-opening tests under displacement-controlled loading.

During the crack initiation tests, the beams were between 116 and 496 days old. In three of the single crack series beams (SC-UC-3, SC-06-14 and SC-22-14-R1), the crack re-opening tests were followed by "near-ultimate" tests where the beams were loaded to 90 kips (400 kN). Three beams (SC-06-08, SC-16-14 and SC-22-08) were tested to ultimate loading after crack re-opening tests. Beams SC-UC-1, SC-22-14 and SC-22-14-R2 were subjected to cyclic tests after the flexural crack initiation and re-opening tests. The multiple crack series beams were only subjected to flexural crack initiation and crack re-opening tests.

STATIC TEST RESULTS

Strain Distribution Through Beam Depth

The existence of pre-release cracks resulted in changes in strain distributions in the vicinity of the cracks compared to the linear strain distributions expected to develop in uncracked specimens. The strains measured during the experimental study represented the superimposed strains due to applied load, with positive strains indicating tension. It should also be noted that all loads referred to in the remainder of this paper are the loads applied by the actuator (the load at each of the two load points is half of this value). The total load carried by the beams was equal to the actuator load plus the self-weight of the beams.

Fig. 5 shows the measured strain distributions along the section 2 in. (51 mm) away from the pre-release crack location for Beam SC-16-08, which had a single nominally 16 in. (406.4 mm) deep, 0.008 in. (0.20 mm) wide pre-release crack. Also shown in Fig. 5 are the strain distributions measured in the uncracked Beam SC-UC-2. Locations of the strain gauges with respect to the nominal pre-release crack geometry in Beam SC-16-08 are shown in an inset in Fig. 5. Comparison of the closing behavior of pre-release cracks in the test beams and in the finite element models indicated that the actual geometry of the cracks produced in the test beams was more nearly a V-shape than that shown in the inset.

Tensile strains near the bottom of Beam SC-16-08 increased significantly below the pre-release crack. This was due to the applied load being carried by the uncracked portion of the section below the pre-release crack at the pre-release crack section. The reduced moment of inertia at the pre-release crack section resulted in increased compressive strains near the pre-release crack tip. It should be noted that these changes in the strain profiles of the sections around the pre-release crack, which are due to the reduced sectional stiffness, are locked-in, and their effect will exist even after the pre-release crack closes completely.

The original depth of the pre-release crack in Beam SC-16-08 was 16 in. (406 mm). As shown in Fig. 5, the gauges placed within the top 14 in. (356 mm) did not measure any appreciable strain for the 4 and 8 kip (17.8 and 35.6 kN) loads, indicating that the pre-release crack remained open under those loads. As the load was increased, the crack closed from the bottom towards the top. At 20 kips (89 kN), the top of the crack still remained open.

Fig. 6 shows the calculated strain distribution for Beam SC-16-08 using the ABAQUS model. The strain values are shown for the elements centered 2 in. (51 mm) away from the cracked section, as indicated. The calculated strain distributions in this figure compare closely to the measured values shown in Fig. 5.

The measured strain distributions for Beams SC-22-14 and SC-UC-2 along sections 2 and 15 in. (51 and 381 mm) away from midspan are shown in Fig. 7. The results for Beam SC-22-14 with a nominal 22 in. (559 mm) deep 0.014 in. (0.36 mm) wide pre-release crack were similar to those of Beam SC-16-08 (Figs. 5 and 6), except for the location of the compressive strain concentration relative to the pre-release crack tip. As shown in Fig. 7(a), the compressive strain concentration occurred well above the level of the crack tip in Beam SC-22-14. This was because the pre-release crack was already partially closed under the effect of beam self-weight.

It is evident from the comparison of Figs. 7(a) and 7(b) that as distance from the pre-release crack increased along the span length, the strain distribution approached that of an uncracked beam. At the section 15 in. (381 mm) away from the pre-release crack, the strain distribution near the bottom of the beam was closer to that of the uncracked beam than the strain distribution near the top. This strain distribution resulted from the top of the pre-release crack remaining open during loading.

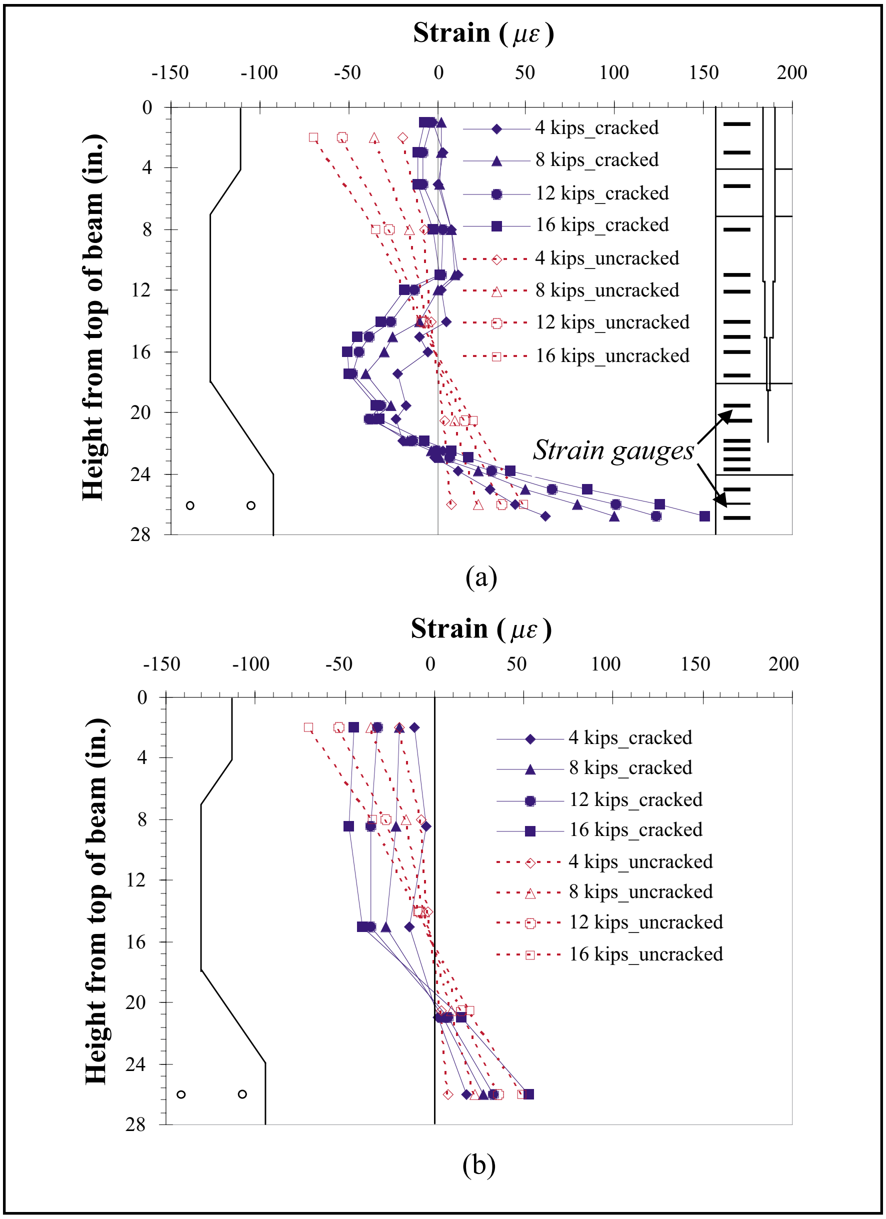

Fig. 7. Comparison of measured strain distributions in beams with and without pre-release crack (Beams SC-22-14 and SC-UC-2): (a) Near pre-release crack; (b) 15 in. (381 mm) away from pre-release crack.

Strain Distribution Along Beam Length

Fig. 8 shows the bottom fiber concrete strains plotted with respect to gauge distance from the pre-release crack location at the beam centerline for Beam SC-22-14 and for uncracked Beam SC-UC-2. The influence of the pre-release crack on the bottom fiber strain distribution is evident in Fig. 8. As expected, there is a uniform strain distribution along the length of the uncracked Beam SC-UC-2 in the constant moment region.

The increase in superimposed tensile strain below the pre-release crack in Beam SC-22-14 was due to the reduced moment of inertia at the section of the pre-release crack. The strain effect was maximum directly below the pre-release crack, and decayed with distance from the cracked section. This strain behavior was also observed for other beams with pre-release cracks, including Beam SC-06-14 shown in Fig. 9. Beam SC-06-14 had the smallest crack depth used in the test beams [6 in. (152 mm)].

The results shown in Figs. 8 and 9 illustrate that among beams incorporating pre-release cracks, beams with deeper pre-release cracks undergo larger strain changes near the pre-release crack location. This occurs because the depth of the uncracked portion of the section below the pre-release crack is smaller for beams with deeper pre-release cracks.

The width of the pre-release crack determines how long the pre-release crack will remain open (and hence how much load will be carried by the section with a reduced moment of inertia). Therefore, pre-release crack width also has an effect on the amount of strain change. The beams with larger pre-release crack widths have larger strain changes than the beams with smaller crack widths for the same pre-release crack depth.

The portion of the span length over which the pre-release cracks had an effect on the bottom fiber concrete

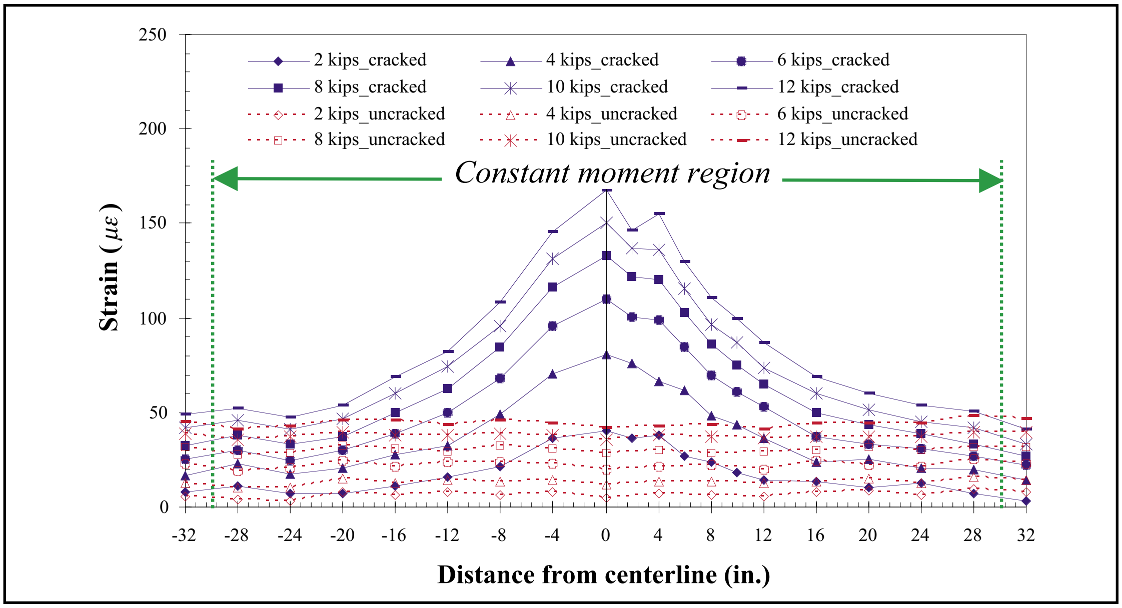

Fig. 8. Comparison of bottom fiber strain distributions along beam length in beams with and without pre-release crack (Beams SC-22-14 and SC-UC-2).

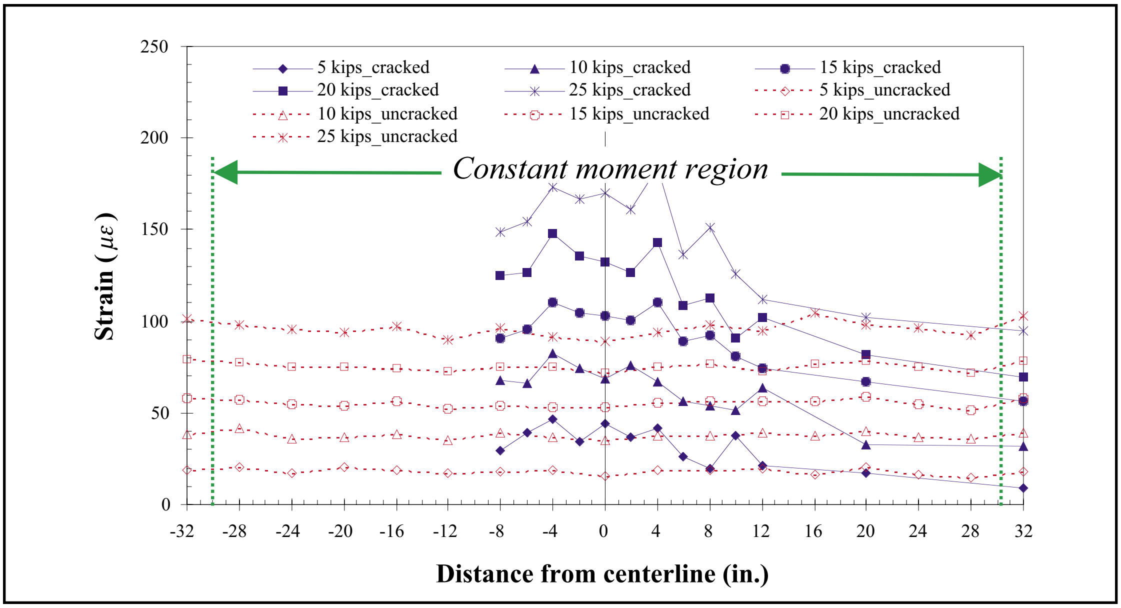

Fig. 9. Comparison of bottom fiber strain distributions along beam length in beams with and without pre-release crack (Beams SC-06-14 and SC-UC-2).

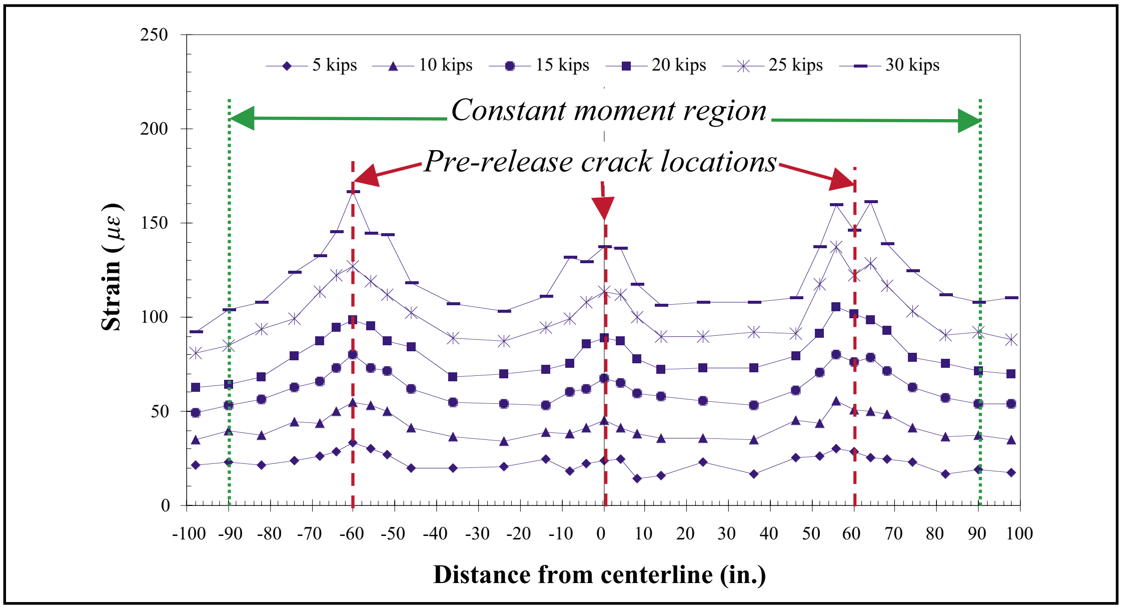

Fig. 10. Bottom fiber strain distributions along beam length for a multiple crack series beam (Beam MC-3C-W).

strains was longer for the deeper [22 in. (559 mm) deep] crack than for the shallower [6 in. (152 mm) deep] crack (see Figs. 8 and 9). While the deeper cracks tended to have a longer affected length, the affected length of the pre-release cracks was limited to a distance equivalent to the depth of the beam on each side of the crack, which was consistent with the finite element models.

The strain profiles shown in Fig. 8 for Beam SC-22-14 became closer to each other in the vicinity of the pre-release crack as the load increased [each line represents a 2 kip (8.9 kN) increase in load], indicating that the beam stiffness increased with increasing load. This stiffening of the beam was due to the closing of the pre-release crack and consequent increase in the local moment of inertia of the cracked section with increasing load.

Such stiffness increase did not occur in Beam SC-06-14 because of the larger resistance to pre-release crack closure. The original stiffness of the cracked section in Beam SC-06-14 was relatively large, so any increase in stiffness due to pre-release crack closure did not change the stiffness markedly.

Bottom fiber concrete strain distributions in the multicrack Beam MC-3C-W are given in Fig. 10. This beam had three pre-release cracks spaced at 60 in. (1524 mm). Bottom fiber tensile strain concentrations were localized in the vicinity of the pre-release cracks as shown in Fig. 10. There was no significant interaction between the affected areas of the pre-release cracks.

The reason that the increases in tensile strains below the pre-release cracks shown in Fig. 10 are smaller than those shown in Figs. 8 and 9 was attributed to the fact that the pre-release crack widths in multiple crack series beams were observed to be much narrower than those in the single crack series beams, although similar crack formers were used to generate the cracks in both series of beams. The effect of smaller pre-release crack widths in multiple crack series beams on the flexural crack initiation and re-opening loads of the beams is discussed later in the paper.

As shown in Fig. 10, the three pre-release cracks caused different amounts of increase in tensile strains. This was

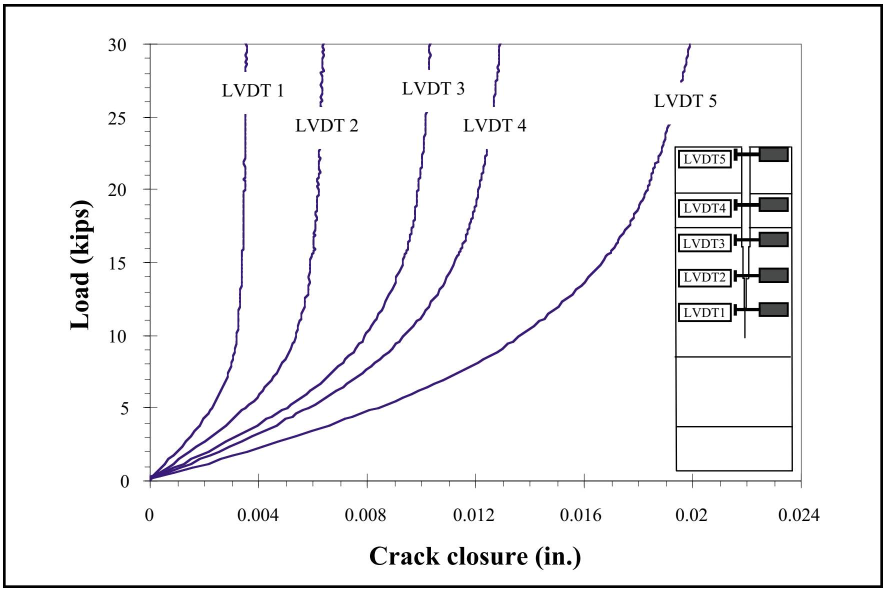

Fig. 11. Closing of pre-release crack determined by LVDTs (Beam SC-16-14).

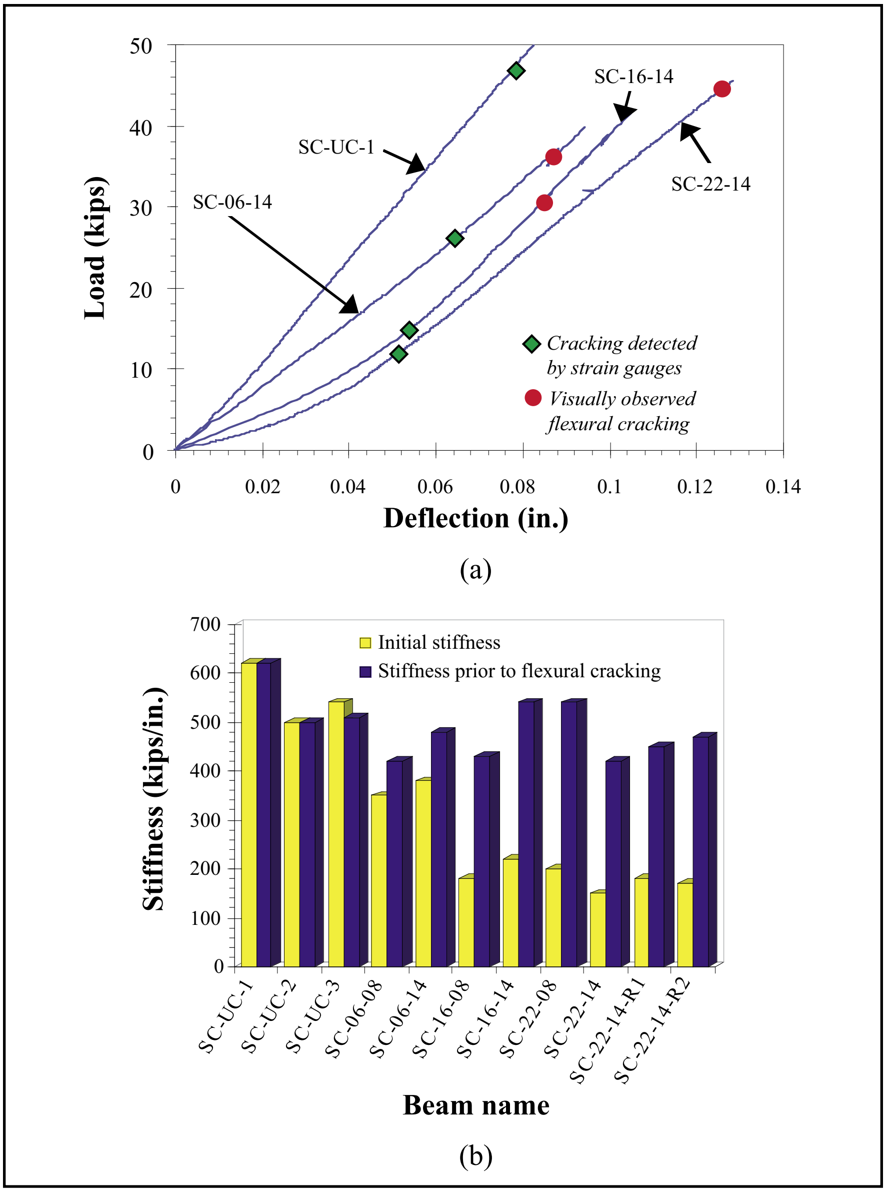

Fig. 12. Effect of pre-release cracks on beam stiffness.

likely due to the difference in the crack geometries, even though the nominal crack geometries were the same as they were made with similar crack formers.

Pre-Release Crack Closure and Beam Stiffness

It was reported in earlier studies that pre-release cracks that developed during the production of precast, prestressed concrete bridge girders were observed to disappear following the release of prestressing strands. Unlike cases observed in the field, the cracks in the test beams did not close completely during the release of prestressing strands due to the relatively small self-weight of the beams together with the relatively large eccentricity of the prestressing force [the prestressing strands in the test beams were located in one row 2 in. (51 mm) from the beam bottom].

In the test beams, the cracks closed by different amounts under the externally applied load depending on the crack geometry. Closure of the pre-release cracks was monitored by LVDTs placed across the cracks at several heights.

Closure of the pre-release crack in Beam SC-16-14 with the applied load during the flexural crack initiation test is shown in Fig. 11. LVDTs used to monitor pre-release crack closure measured the deformations due to compressive strains over the gauge length as well as the deformations due to crack closure. As the former part of the measured displacement was negligible compared to the latter part, the change in displacements measured by the LVDTs provided a good estimate of the pre-release crack closure.

The plot for each LVDT exhibited nonlinear behavior during the pre-release crack closure, followed by linear behavior after the pre-release crack closed completely. During the nonlinear portion, there was a continuous increase in the stiffness of the cracked section, as shown in Fig. 11. As the response of the beam is affected by the pre-release crack closure, the same type of behavior (i.e., nonlinear portion during crack closure followed by linear portion after the crack closed completely) was also observed in other measured quantities, including midspan deflection and concrete strains.

Load versus midspan deflection plots of the beams measured during flexural cracking tests are presented in Fig. 12(a) for an uncracked beam and beams with nominal pre-release crack widths of 0.014 in. (0.36 mm). The beams with 16 and 22 in. (406 and 559 mm) deep pre-release cracks exhibited nonlinear load versus midspan deflection behaviors.

As explained above, the nonlinear response of the beams was due to closure of the pre-release cracks during loading. Beam SC-06-14 exhibited a different behavior than the other two beams incorporating pre-release cracks (Beams SC-16-14 and SC-22-14). The small depth of the pre-release crack in Beam SC-06-14 compared to the beam depth resulted in pre-release crack closure values that were not large enough to affect the linear behavior of load-displacement response of the beam.

A comparison among the measured initial stiffnesses and those prior to flexural cracking of the beams is presented in Fig. 12(b). The stiffness values shown represent the slopes of the initial and final portions of the load versus midspan deflection plots obtained during the flexural cracking tests [Fig. 12(a)]. To determine the "final stiffnesses" of the beams, the visually observed flexural cracking loads, rather than the cracking loads from the strain gauges, were used as the limit.

This is because when the flexural cracking was detected by the strain gauges, the cracks were only small surface cracks and did not cause a change in the overall beam stiffness until they became visible. A detailed compari-

Table 3. Measured flexural cracking and crack re-opening loads of the single crack series beams.

Beam designation	Visually observed cracking load, kips	Cracking load from bottom fiber strains, kips	Distance of first observed crack(s) from midspan,† in.	Crack re-opening load from bottom fiber strains, kips	Crack re-opening load from LVDTs, kips	Ultimate capacity,‡ kips
SC-UC-1*	67	47	-20, 16, 24	27	27	Not tested
SC-UC-2*	64	29	18	n/a	26	Not tested
SC-UC-3*	57	44	7	n/a	26	Not tested
SC-06-08	40	19	1	10	n/a	142
SC-06-14	37	26	1	9	10	Not tested
SC-16-08	25	n/a	3	n/a	8	Not tested
SC-16-14	32	15	1	6	5	143
SC-22-08	36	19	2	3	6	138
SC-22-14	45	12	1	4	4	Not tested
SC-22-14-R1	31	15	2	n/a	4	Not tested
SC-22-14-R2	35	12	1	n/a	4	Not tested

* Indicate beams without pre-release cracks.
† Constant moment region extended 30 in. on both sides of midspan.
‡ The predicted ultimate capacity for an uncracked beam was 134 kips.
n/a: Flexural crack initiation or re-opening load for this beam could not be determined.
Note: 1 in. = 25.4 mm; 1 kip = 4.448 kN.

son of flexural cracking loads from the strain gauges and from visual observations is given in the following section.

The difference among the stiffnesses of the uncracked beams (Beams SC-UC-1 through SC-UC-3) in Fig. 12(b) may be partially due to the change in the modulus of elasticity of the concrete during the testing program. Beam SC-UC-1 was subjected to the cracking test approximately 9 months after the tests for Beams SC-UC-2 and SC-UC-3 (Beams SC-UC-2 and SC-UC-3 were approximately 4.5 and 4 months old, respectively, when subjected to load testing).

Fig. 12(b) clearly shows that the initial stiffnesses of the beams incorporating pre-release cracks were always smaller than the stiffnesses of the beams without pre-release cracks. Due to closure of the pre-release cracks, the final stiffness of the beams with pre-release cracks increased and approached the stiffness of the beams with no cracks. Initial and final stiffnesses of the beams with 6 in. (152 mm) deep cracks were similar to each other, suggesting that these cracks closed less than the others during loading.

Flexural Crack Initiation and Re-Opening Loads

Two methods were used to determine the flexural crack initiation loads: visual observation and use of the bottom fiber strain data. A third method, use of crack detection gauges, did not provide a reliable means to determine flexural cracking and these results were not considered.

In determining the initiation of flexural cracking from the bottom fiber strain data, a relief or a sudden increase in the measured tensile strains — depending on the relative positions of the strain gauge and the flexural crack — was taken as an indication of flexural crack initiation. A detailed description of the method can be found in Baran et al.[9] The visually observed flexural cracking loads for all beams were larger than the flexural crack initiation loads determined from the strain gauges. As the visually observed cracking loads are the loads at which the flexural cracks became wide enough to be visible by a naked eye, these loads represent an upper bound for the flexural crack initiation loads of the beams.

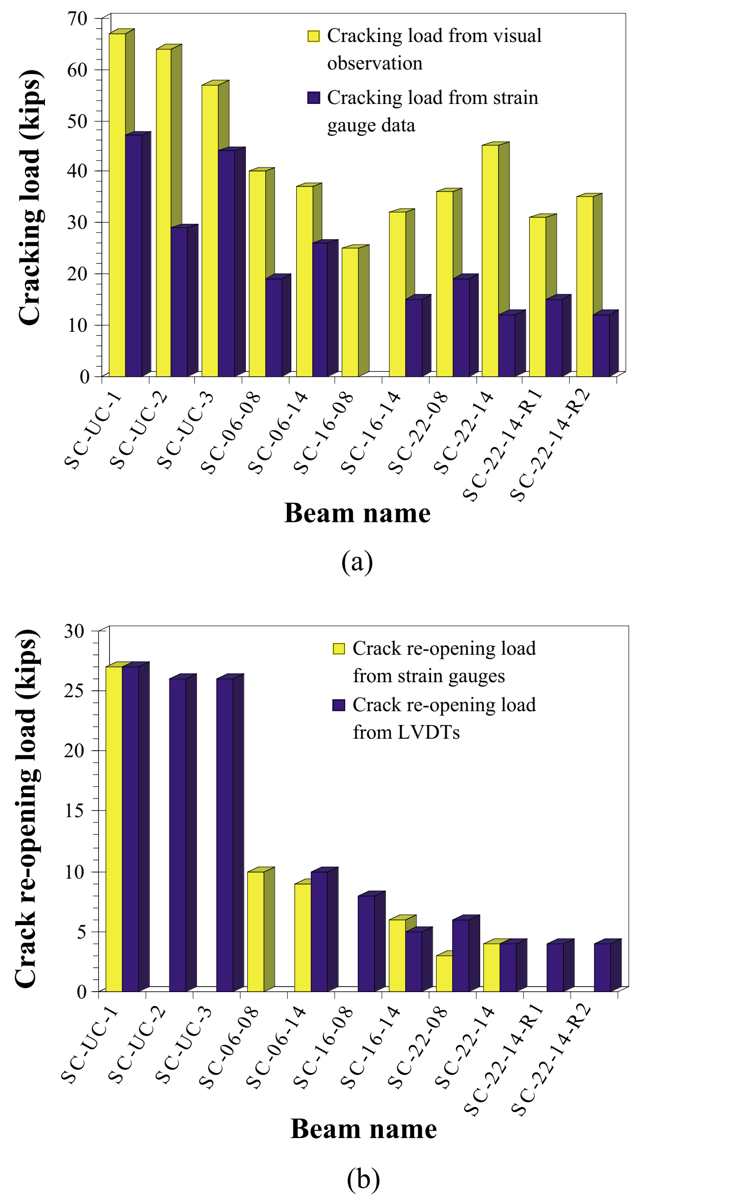

Fig. 13. Comparison of flexural cracking: (a) Crack initiation; (b) Crack re-opening (note the scale difference).

A similar procedure was used to determine flexural crack re-opening from the bottom fiber strain data (i.e., flexural crack re-opening load was taken as the load at which the slope of the load versus bottom fiber strain plots changed). LVDTs placed over and next to the major flexural cracks at the bottom surface of the beams after the crack initiation tests provided another means to measure flexural crack re-opening. In this case, the load at which the initial slope of the load-versus-displacement plot changed was taken to be the crack re-opening load.[9]

Flexural crack initiation and re-opening loads of the single crack series beams are tabulated in Table 3 together with the associated location of the flexural cracks. Cracking loads in Table 3 show that the beams incorporating pre-release cracks had smaller flexural cracking loads than the beams without pre-release cracks.

This is also illustrated in the bar chart of Fig. 13(a), which provides a comparison of cracking loads obtained from the bottom fiber strain data and from visual observation. Flexural crack initiation and re-opening loads of Beam SC-UC-2 were almost identical, suggesting that this beam had already

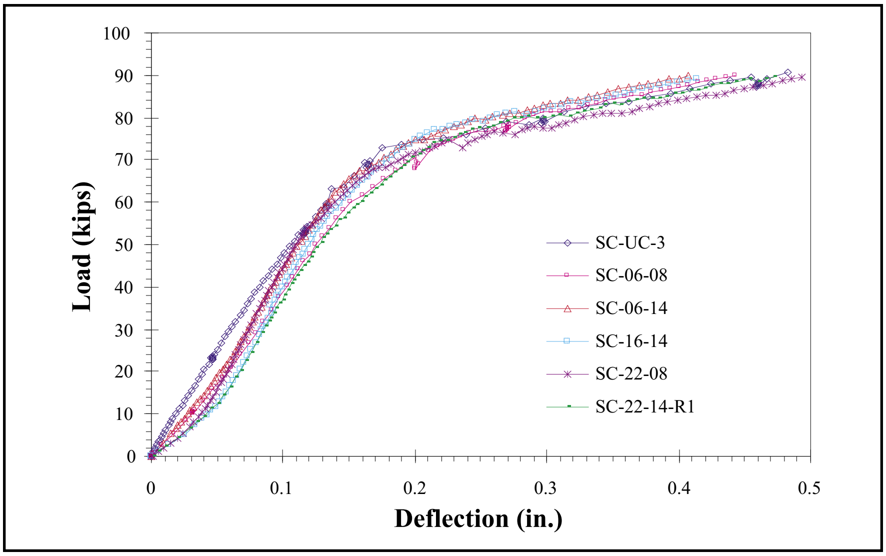

Fig. 14. Load versus midspan deflection at near-ultimate load tests.

been flexurally cracked prior to the load tests.

As shown in Table 3, the locations of the first flexural crack observed in the beams incorporating pre-release cracks were localized in a region at most 3 in. (76 mm) from the pre-release crack (i.e., midspan of beams); whereas, in the initially uncracked beams, the first flexural cracks were spread over the constant moment region. The difference in the location of first flexural cracking between the beams with and without pre-release cracks was attributed to the localized effects of the pre-release cracks.

Fig. 13(b) shows the flexural crack re-opening loads determined from the bottom fiber strain data and LVDT readings (also see Table 3). For the beams where the crack re-opening load could be determined from both strain gauges and LVDTs, these loads were in good agreement. Crack re-opening loads for the beams without pre-release cracks (Beams SC-UC-1, SC-UC-2 and SC-UC-3) were all significantly larger than the crack re-opening loads of the beams with pre-release cracks.

The pre-release cracks in the single crack series test beams did not close completely at flexural crack initiation and re-opening loads. As explained earlier, the reduction in the flexural crack initiation and re-opening loads of the beams with pre-release cracks was due to two effects:

The first effect was the reduced compressive strains at the bottom of the beams below the pre-release cracks that were "locked in" during the closure of the pre-release cracks.

The second effect was the reduced sectional stiffness at the pre-release crack locations caused by the cracks remaining partially open.

It was not possible to measure the individual contributions to reduced flexural crack initiation loads caused by these two effects. However, an analysis of experimental data was performed to approximate the separate effects of these two factors.

For the single crack series test beams, the depth of the part of the pre-release cracks that remained unclosed at flexural crack initiation load was determined using the measured pre-release crack closure values. Using these depth values, the cracking capacity of the concrete section below the open part of pre-release cracks was calculated. It should be noted that the amount of prestressing force and the tensile strength of concrete values used in the calculations were calibrated such that the predicted flexural crack initiation and re-opening loads of beams with no pre-release cracks were the same as those obtained from the experiments.

The difference between the calculated cracking capacity of an originally uncracked beam and the cracking capacity calculated considering the concrete section below the open part of pre-release crack was the reduction in flexural cracking load due to the "second effect" mentioned above (reduction in sectional stiffness due to pre-release cracks remaining partially open). Because the total reduction in flexural cracking load under the two effects together was known (the difference between the measured cracking loads of beams with and without pre-release cracks), the reduction due to the "first effect" mentioned above (reduced bottom fiber compressive strain due to pre-release crack closure) on flexural cracking loads was obtained as the difference between the total measured reduction and the calculated reduction due to the pre-release cracks remaining partially open.

For each beam in the single crack series tests, the reduction in flexural cracking loads due to these two separate effects was approximated with the procedure explained above. The results indicated that for most of the beams, the major part of the reduction in flexural cracking loads was due to the reduced moment of inertia caused by the pre-release cracks remaining partially open. However, there were also cases for which the "locked in" effect of the reduced bottom fiber stresses due to pre-release crack closure was as much as the effect caused by the cracks remaining partly open.

For example, a total reduction in flexural cracking load of 28 kips (125 kN) was measured for Beam SC-06-08, and 15 kips (67 kN) of the total reduction was determined to be due to the reduced moment of inertia caused by the pre-release crack remaining partially open. The remaining 13 kips (58 kN) reduction in the flexural cracking load of this beam was due to the reduced compressive strains at the bottom of the beam below the pre-release crack that were "locked in" during the closure of the pre-release crack.

This behavior is consistent with the previously mentioned finite element result: existence of pre-release cracks might cause unacceptably large changes in beam stresses even if the cracks close under the effects of prestressing force and beam self-weight, and remain closed under external loading. Results from a previous study also provide experimental validation of this finding.[1] As mentioned earlier, the pre-release cracks in one of the full-scale prestressed concrete girders tested by

Ahlborn et al.[1] were observed to close completely following strand release and the flexural cracking capacity of the girder was reduced.

For the 30 ft (9.14 m) beams, there was a negligible difference in behavior between the beams without pre-release cracks and with single and multiple pre-release cracks. Although similar crack formers were used to generate the pre-release cracks in the 30 ft (9.14 m) beams, the crack widths in these beams appeared to be much narrower than those in the 20 ft (6.1) beams.

The reason for the negligible difference in flexural cracking loads among the 30 ft (9.14 m) beams was attributed to smaller realized pre-release crack widths than the anticipated crack widths, which resulted in complete closure of the pre-release cracks in these beams prior to flexural crack initiation and re-opening. As the pre-release cracks closed completely prior to flexural crack initiation and re-opening, the "second effect" explained above (i.e., reduced sectional stiffness) was not observed for these beams, and any reduction in flexural crack initiation load of these beams was due to the reduced bottom fiber compressive stress caused by pre-release crack closure alone.

Discussion on Flexural Crack Initiation and Re-Opening Loads

The flexural crack initiation and re-opening loads for the 20 ft (6.1 m) beams without pre-release cracks were calculated to be 70 and 39 kips (311 and 174 kN), respectively. Measured quantities of 104,500 lbs (465 kN) and 650 psi (4.5 MPa) were used in the calculations for the prestressing force and concrete modulus of rupture, respectively.

The effective prestress immediately after the load testing of the beams was experimentally determined in Beams SC-UC-3, SC-22-14-R1, MC-UC-1, and MC-1C. In each of these beams, two of the strands were exposed over a short length by removing the concrete at the corner of the bottom flange on both sides of the beams. The exposed lengths of the strands were approximately 20 in. (508 mm) at a distance approximately 50 in. (1270 mm) from the ends of the beams. Each strand was flame-cut after being instrumented with strain gauges. To determine the effective prestress from the measured strain data, modulus of elasticity values measured from "in-air" strand tests were used.

The average of the measured flexural crack initiation and re-opening loads of the 20 ft (6.1 m) beams without pre-release cracks were 46 and 26 kips (205 and 116 kN), respectively. The reason for the measured flexural crack initiation and re-opening loads being smaller than the predicted values may be attributed to effects such as restrained concrete shrinkage at the bottom surface

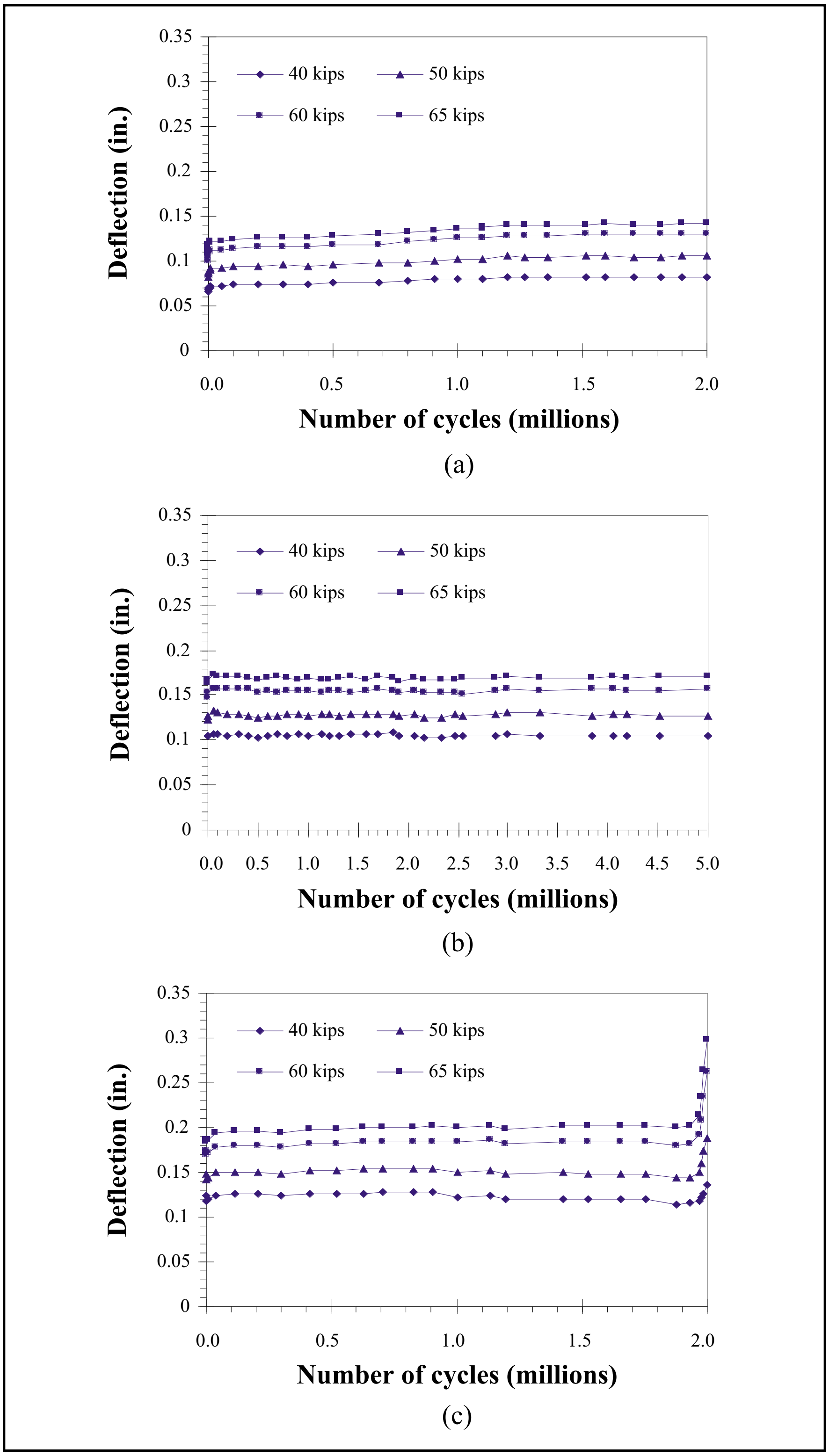

Fig. 15. Midspan deflection versus number of cycles: (a) Beam SC-UC-1; (b) Beam SC-22-14; (c) Beam SC-22-14-R2.

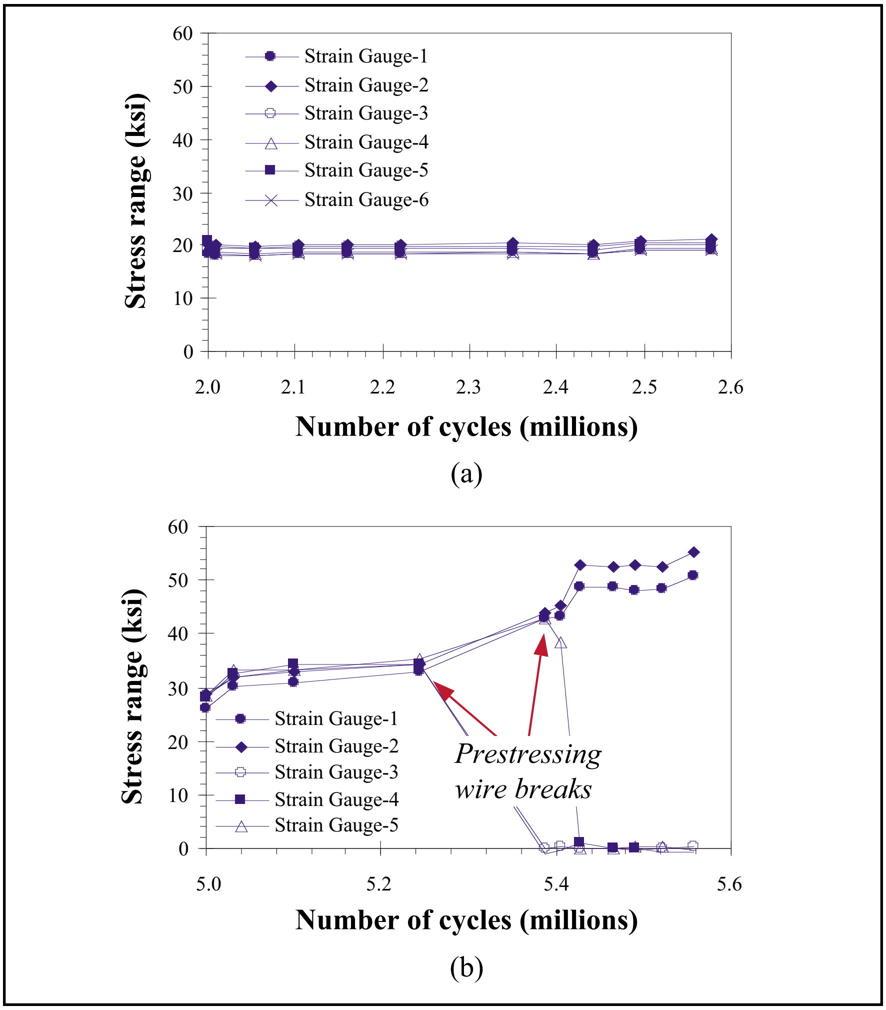

Fig. 16. Strand stress range versus number of cycles: (a) Beam SC-UC-1; (b) Beam SC-22-14.

of beams by the core concrete, an effect not accounted for in the predicted cracking loads.

Data reported in earlier studies indicated similar discrepancies between the calculated and experimentally obtained flexural crack initiation loads.[10-12]

Ultimate Load

Results from testing of three of the beams with different size pre-release cracks (Beams SC-06-08, SC-16-14, and SC-22-08) to failure indicated that the ultimate load of the beams was independent of the crack geometry. Moreover, as presented in Table 3, the measured ultimate flexural capacities of the three beams tested with various pre-release crack sizes were approximately the same as the predicted capacity of an uncracked beam, which was calculated using an iterative procedure with the strand stress-strain relation given in the PCI Design Handbook.[13] These results indicate that the existence of pre-release cracks did not have an effect on the ultimate flexural capacity of the beams.

Fig. 14 shows a comparison of the load versus midspan deflection obtained during the near-ultimate load tests, where the beams were loaded up to 90 kips (400 kN). Near-ultimate state tests created similar patterns of flexural cracks in the beams, irrespective of the presence or absence of a pre-release crack, and irrespective of the pre-release crack size. As seen in Fig. 14, there was no significant difference among the responses of the beams, except in initial beam stiffnesses, which was discussed earlier.

CYCLIC TEST RESULTS

Following the flexural crack initiation and re-opening tests, three of the single crack series beams (Beams SC-22-14, SC-22-14-R2, and SC-UC-1) were subjected to cyclic tests. The maximum loads to which the beams were subjected to during the flexural crack initiation tests were 45, 46, and 67 kips (200, 205 and 298 kN), respectively. Prior to cyclic tests, the flexural cracks were only visible at the bottom surface of the beams.

The load ranges used in the cyclic tests were chosen in consultation with Mn/DOT Bridge Office. During the cyclic tests, the beams were cycled in load control under four-point bending between 39 and 67 kips (174 and 298 kN). A loading rate of 1.6 Hz was used throughout the cyclic tests. The 67 kip (298 kN) maximum load corresponded to a nominal bottom fiber tensile stress of $6\sqrt{f'_c}$ for a beam with no pre-release cracks, where f'_c was the measured compressive strength of the concrete.

With the minimum load level of 39 kips (174 kN), flexural cracks in a beam with no pre-release cracks were expected to undergo crack re-opening. The strand stress range corresponding to these load levels was calculated to be 23.4 ksi (161.3 MPa) based on a partially cracked section with no pre-release cracks. For the same load range, the calculated strand stress range in an uncracked section was 2.8 ksi (19.3 MPa).

Beams SC-22-14 and SC-UC-1 were taken through 5 million and 2 million cycles, respectively, of fatigue loading before pausing the testing with no significant degradation in beam stiffnesses. The change in static midspan deflection of beams with increasing number of cycles is shown in Fig. 15. As evident from the plots, Beams SC-22-14 and SC-UC-1 exhibited stable behavior, even though Beam SC-UC-1 shows a very slight reduction in stiffness.

After 5 million and 2 million load cycles, respectively, a short length of strand in Beams SC-22-14 and SC-UC-1 was exposed and instrumented with strain gauges in the vicinity of the major flexural cracks. The strain data from these gauges was used to determine strand stress ranges during continued cyclic tests.

Measured changes in strand stress ranges in these beams are shown in

Fig. 16. The strand stress ranges in Beam SC-UC-1 remained constant at approximately 20 ksi (138 MPa) with no wire breaks during the 580,000 load cycles following the initial 2 million cycles of testing. In Beam SC-22-14, on the other hand, wire fractures were observed at 390,000 and 430,000 load cycles after the initial 5 million cycles of loading. The strand stress ranges in this beam were measured to be 35.3 and 43.9 ksi (243.3 and 302.7 MPa), respectively, before the first and the second wire breaks.

Cyclic testing of Beam SC-22-14-R2, which was a replicate of Beam SC-22-14, was terminated after 2 million load cycles due to excessive deformations. As shown in Fig. 15(c), the beam stiffness deteriorated rapidly after approximately 1.9 million cycles. After 2 million cycles, there were two fractured wires in one of the edge strands below the pre-release crack. All seven wires in the same strand were observed to be fractured approximately 12 in. (305 mm) from the pre-release crack location.

CONCLUSIONS

A combination of static and cyclic tests on full-scale precast, prestressed concrete beams was conducted to evaluate the effect of the existence of vertical pre-release cracks. Experimental results[9] obtained from the static tests validated the results of the finite element study.[7]

Unlike cases observed in the field, the pre-release cracks in the test beams did not close completely under the effects of beam self-weight and prestressing force due to (1) relatively small self-weight moment of the beams due to the small cross-sectional area and short span length and (2) large resistance against pre-release crack closure caused by the relatively large eccentricity of the prestressing force used in the beams. The fact that the pre-release cracks remained open prior to load testing of the beams provided the opportunity to monitor the closing of the cracks during load tests.

The reduction in the flexural crack initiation and re-opening loads observed in the finite element models and the test beams was due to two effects. Part of the reduction was attributed to the reduction in bottom fiber compressive stresses below the pre-release cracks due to closing of the cracks; and the remaining part was due to the reduced sectional stiffness at the pre-release crack locations when the cracks remained partially open at the flexural crack initiation and re-opening loads. Although the latter effect caused the major reduction in flexural cracking loads, the effect due to the "locked in" stresses due to pre-release crack closure was not negligible and in several cases was comparable to the effect of the reduced moment of inertia.

The following conclusions were drawn from this study:

1. The existence of pre-release cracks affected the strain distributions through the beam depth. The changes included reduced bottom fiber compressive strains below the pre-release crack, reduced compressive strains at the top of the crack, and increased compressive strains near the crack tip. The reduced compressive strains below the cracks resulted in lower flexural crack initiation and re-opening loads for beams incorporating pre-release cracks than for beams that did not have pre-release cracks. The overall stiffnesses of the beams were also affected by the reduction in the moment of inertia of the pre-release crack section.
2. Even though following the closure of the pre-release cracks the stiffness of the original uncracked beams was recovered, the effects caused by the existence of pre-release cracks on beam stresses during crack closure were "locked in." This "locked in" condition indicates that even if the pre-release cracks close completely on the precasting bed under the effects of beam self-weight and the prestressing force, the stress distributions near the crack locations will be different than those of originally uncracked beams.
3. Due to the strain changes caused by the existence of pre-release cracks, a nonlinear strain distribution occurred near the pre-release cracks during crack closure. The nonlinearity of the strain distribution decreased as the horizontal distance from the pre-release cracks increased. The effect of the cracks decayed almost completely at a distance equal to the depth of the beam on either side of the cracked section. The amount of strain changes and the affected areas in the beams were dependent on the size of the pre-release cracks. In general, deeper and wider cracks resulted in larger effects.
4. No significant difference could be detected between the near-ultimate behavior of the beams with and without pre-release cracks. In addition, there were only marginal differences between the measured ultimate flexural capacities of the beams involving different size pre-release cracks.
5. The limited cyclic test results indicated that a beam that develops pre-release cracks may be more likely to experience fatigue problems than a beam with no pre-release cracks. In this particular study, the beams were subjected to cyclic testing in the cracked state. If the maximum load to which the beams were subjected during cyclic tests was smaller, then the beam with no pre-release cracks might have remained flexurally uncracked while the beam with the pre-release crack might have undergone flexural cracking due to the effect of the pre-release crack. In this loading scenario, the difference between the fatigue behaviors of the beams with and without pre-release cracks would have been more significant.

Even though the results obtained in this study indicated that the existence of pre-release cracks causes a reduction in the flexural cracking load of prestressed concrete bridge girders, there are factors that will tend to reduce the negative effects of pre-release cracks and cause the girders to remain uncracked under service loads. The two possible sources of reserve flexural cracking capacity of prestressed concrete bridge girders are (1) as-built concrete strengths that are higher than the specified design values and (2) conservative distribution factors used to calculate the loads on an individual girder. These factors will tend to neutralize the negative effects caused by the existence of pre-release cracks as they would increase the flexural cracking load above the design value. Positive measures that may be taken to reduce the occurrence of pre-release cracks may include the avoidance of short free lengths of strand between girders during production and avoidance of a prolonged period of time between form stripping and releasing the prestressing strands.

ACKNOWLEDGMENTS

The research documented in this paper was sponsored by the Minnesota Department of Transportation. Their support is gratefully acknowledged. The authors also wish to acknowledge the Minnesota Supercomputing Institute for the use of the computer software ABAQUS.

Special thanks are due to Mike Dorval and other staff of Elk River Concrete Products for their cooperation and assistance during fabrication and transportation of the test beams.

The findings and opinions expressed in this paper are those of the authors only, and do not necessarily represent the views of the sponsoring agencies.

Finally, the authors wish to express their appreciation to the PCI JOURNAL reviewers for their constructive comments.

REFERENCES

1. Ahlborn, T., French, C., and Shield, C., "High-Strength Prestressed Concrete Bridge Girders," Minnesota Department of Transportation, Research Report MN/RC-2000-32, 2000, St. Paul, MN.
2. Roller, J. J., Martin, B. T., Russell, H. G., and Bruce, R. N., "Performance of Prestressed High Strength Concrete Bridge Girders," PCI JOURNAL, V. 38, No. 3, May-June 1993, pp. 34-45.
3. Roller, J. J., Russell, H. G., Bruce, R. N., and Martin, B. T., "Long-Term Performance of Prestressed, Pretensioned High Strength Concrete Bridge Girders," PCI JOURNAL, V. 46, No. 6, November-December 1995, pp. 48-59.
4. Green, J. K., Cookson, P. J., and Johnson, K. A. L., "The Performance of Pretensioned Concrete Beams That Have Cracked Before Transfer of Prestress," *The Structural Engineer*, V. 62B, No. 4, December 1984, pp. 79-85.
5. Zia, P., Kowalsky, M. J., Ellen, G. C., and Longo, S. E., "Fatigue Testing of Two Full-Size Pre-Cracked AASHTO Bridge Girders," Large-Scale Structural Testing, SP 211, 2003, American Concrete Institute, Farmington Hills, MI, pp. 1-16.
6. Zia, P., and Caner, A., "Cracking in Large-Sized Long-Span Prestressed Concrete AASHTO Girders," North Carolina Center for Transportation Engineering Studies, Research Report FHWA/NC/94-003, 1993, Raleigh, NC.
7. Wyffels, T., French, C., and Shield, C., "Effects of Pre-Release Cracks in High-Strength Prestressed Girders," Minnesota Department of Transportation, Research Report MN/RC-2000-25, 2000, St. Paul, MN.
8. Hibbit, Karlsson & Sorensen, Inc., ABAQUS. Version 5.4, Pawtucket, RI, 1994.
9. Baran, E., French, C., and Shield, C., "Effects of Vertical Pre-Release Cracks on Prestressed Bridge Girders," Minnesota Department of Transportation, Research Report MN/RC-2003-33, 2002, St. Paul, MN.
10. Shanafelt, G. O., and Horn, W. B., "Guidelines for Evaluation and Repair of Prestressed Concrete Bridge Members," National Cooperative Highway Research Program Research Report 280, 1985, Transportation Research Board, Washington, DC.
11. Shenoy, C. V., and Frantz, G. C., "Structural Tests of 27-Year-Old Prestressed Concrete Bridge Beams," PCI JOURNAL, V. 36, No. 5, September-October 1991, pp. 80-90.
12. Halsey, J. T., and Miller, R., "Destructive Testing of Two Forty-Year-Old Prestressed Concrete Bridge Beams," PCI JOURNAL, V. 41, No. 5, September-October 1996, pp. 84-93.
13. *PCI Design Handbook – Precast and Prestressed Concrete*, Fifth Edition, Precast/Prestressed Concrete Institute, Chicago, IL, 1999.